3   **Reliability and component importance in networks subject to spatially distributed hazards**

4   **followed by cascading failures**

5   **Anke Scherb[1]**

6   Technische Universität München
7   Theresienstr. 90, 80333 Munich, Germany
8   e-mail: anke.scherb@tum.de

9   **Luca Garrè**

10   DNV GL
11   Veritasveien 1, 1363 Høvik, Norway
12   e-mail: luca.garre@dnvgl.com

13   **Daniel Straub**

14   Technische Universität München
15   Theresienstr. 90, 80333 Munich, Germany
16   e-mail: straub@tum.de

17

18   **Abstract**

19   We investigate reliability and component importance in spatially distributed infrastructure networks

20   subject to hazards characterized by large-scale spatial dependencies. In particular, we consider a selected

21   IEEE benchmark power transmission system. A generic hazard model is formulated through a random

22   field with continuously scalable spatial autocorrelation, to study extrinsic common-cause-failure events

23   such as storms or earthquakes. Network performance is described by a topological model, which

24   accounts for cascading failures due to load redistribution after initial triggering events. Network

25   reliability is then quantified in terms of the decrease in network efficiency and number of lost lines.

26   Selected importance measures are calculated to rank single components according to their influence on

27   the overall system reliability. This enables the identification of network components that have the

28   strongest effect on system reliability. We thereby propose to distinguish component importance related

29   to initial (triggering) failures and component importance related to cascading failures. Numerical

30   investigations are performed for varying correlation lengths of the random field, to represent different

31   hazard characteristics. Results indicate that the spatial correlation has a discernible influence on the

32   system reliability and component importance measures, whilst the component rankings are only mildly

33   affected by the spatial correlation. We also find that the proposed component importance measures

34   provide an efficient basis for planning network improvements.

---

[1] Corresponding author

1 INTRODUCTION

The societal requirements on continuous and reliable power supply are increasing, yet regional blackouts in European and North American power grids have occurred frequently in the last two decades [1]. Short time blackouts alone lead to an estimated annual economic loss of between US$ 104 billion and US$ 164 billion in the USA [2]. In many cases, natural hazards such as earthquakes, windstorms, floods or heat waves are the initial triggering events. Therefore, significant research is ongoing within the broad field of power grid restoration and strengthening against natural hazards. This research includes the modeling of network performance and cascading failure, network or system reliability and component importance, and common cause failures (CCF) in the context of natural hazards.

In system reliability assessments, component importance measures are employed to rank components based on their influence on the overall system reliability. Most importance measures (IMs) currently utilized depend on the component's function in the system and on the reliability of the component in question [3]. The resulting rankings can serve the identification of components to be repaired, strengthened, replaced, or alleviated from external or internal load impacts. Importance measures can further support the improvement of maintenance, operating methods, and network expansion planning. Several studies applied IMs specifically to network reliability analysis for electrical power systems [e.g., 4, 5-9].

Network vulnerability to natural hazards has been assessed and modelled synoptically in a number of studies [10-13]. Large-scale natural hazards, including windstorms or earthquakes, can lead to multiple simultaneous component failures, i.e. CCF. Natural hazards are characterized by spatial distributions and variability, which should be accounted for in the analysis of the reliability and IMs for infrastructure networks. Classical approaches for the modeling of CCF in system and network reliability analysis [e.g., 14, 15, 16] do not consider spatial correlation in CCF. However, models for network reliability analysis under spatially correlated hazards have been developed [e.g., 11-13, 17, 18-23]. These studies focus on scenario-based reliability analyses of specific infrastructures subjected to hazards, but do not systematically investigate and quantify the effects of varying autocorrelation structures on system reliability. Andreasson, et al. [24] analyze a model for the Nordic power grid to study effects of correlated failures of power lines on the total system load shed. They conclude that with increased dependence among line failures, the expected value and the variance of the system load shed increases significantly. Rahnamay-Naeini, et al. [25] model correlated failures as spatial point processes and their effects on network reliability for communication networks in the US. They find that the network performance in terms of network efficiency decreases with increasing degree of correlation among component failures. Both Andreasson, et al. [24] and Rahnamay-Naeini, et al. [25] do not include the effect of cascading failures following initial triggering failure events in the network.

The effect of CCF on the importance of components for system reliability has been studied for general networks by Bérenguer, et al. [26] and Tanguy [27]. The latter assessed the effect of generic CCF models

71 on the system reliability and various IMs in a network with 9 nodes and 14 lines. Tanguy [27] concludes
72 that adding CCF effects to the model of a small sized network does not profoundly change the ranking
73 of the system components. None of these studies investigates how spatial dependence influences the
74 behavior of component importance measures in spatially distributed networks. A first approach in this
75 direction is reported in Scherb, et al. [28], where we focus on the s-t connectivity for network
76 performance assessment. Our results obtained for the IEEE118 bus system show that the spatial
77 dependence should be explicitly considered if the correlation length of the hazard is in the range between
78 the lengths of individual lines to the diameter of the entire system.

79 Our aim is to investigate the reliability and component importance in spatially distributed infrastructures,
80 accounting for the spatial dependence of the exogenous hazard and resulting cascading failure processes.
81 The hazard event is idealized by a spatial random field, which is parametrized through the correlation
82 length. The network is modeled as a complex graph and the network performance under disturbances is
83 quantified through the efficiency measure of Latora and Marchiori [29]. The reliability and component
84 importance rankings are determined in function of this parameter. The IMs are thereby formulated once
85 with respect to failures caused directly by the hazard event, and once with respect to cascading failures.
86 We compare these two IM formulations and find that the distinction made by the two formulations is
87 key to identifying efficient network improvement strategies. Numerical investigations are performed on
88 the IEEE 39 bus benchmark system for transmission power grids.

89 ## 2 METHODS

90 ### 2.1 *Power grid represented as a complex graph*

91 Modeling the performance and assessing the reliability of large infrastructure systems is demanding in
92 terms of both the modeling and the computation efforts, in particular if cascading effects are to be
93 accounted for.

94 To enhance computational efficiency, power grids can be represented as complex weighted graphs [30-
95 33]. Even though the reduction of a power grid to a complex graph leads to a simplified grid description
96 [34], graph theory can provide insights into the degree of connectivity of a power grid and help identify
97 potential critical aspects for a first reliability estimation with a level of accuracy that is comparable to
98 traditional electrical engineering approaches [32, 35-38].

99 Applying a complex graph representation, we describe the power grid by a weighted and undirected
100 graph G, consisting of a set of N nodes (vertices) and a set of K lines (edges). In a graph representation
101 of a power transmission grid, nodes typify generation, transmission, and distribution buses, or
102 substations. Lines model the transmission cables and transformers. The $n \times n$ adjacency matrix $\mathbf{A} =$
103 $\{a_{ij}\}$ of the graph describes its topology. The entry a_{ij} takes value zero if no connection between nodes

104 i and j exist. If there is a link between i and j, the entry a_{ij} is the weight assigned to the line. Here, the

105 reactance values of the transmission lines are used as weights. The reactance of a transmission line is an

106 indicator of the amount of power flowing through a line under the assumption of lossless conditions [39,

107 40]. The lower the reactance of a path between two nodes, the more power may flow through the path.

108 Because the graph is undirected, it is $a_{ij} = a_{ji}$.

2.2 *Network performance and reliability*

110 In network analysis based on graph theory, performance measures are derived from topological

111 properties of networks [40-42]. For instance, Motter and Lai [43] define the load of a node as the total

112 number of shortest paths passing through the node, which corresponds to the *betweenness index*. This

113 load can increase when another node of the network fails, possibly leading to the overloading of

114 additional nodes. The model has been further developed and extended with the concept of graph

115 efficiency [29, 41]. Dwivedi, et al. [40] modified the betweenness index by considering the total number

116 of shortest paths through an edge instead of a node. This modeling approach has been used to model

117 cascading failures in power grids [e.g., 40, 44].

118 2.2.1 *Efficiency of a power network as performance measure*

119 The efficiency of a single line e_{ij} is defined as the inverse of its reactance, a_{ij} (with $a_{ij} > 0$):

$$e_{ij} = \frac{1}{a_{ij}} \left[\frac{1}{\Omega} \right] \tag{1}$$

120 The efficiency of a path between two nodes is the sum of the efficiencies of the lines that constitute the

121 path. In defining the efficiency of the network, it is assumed that the connection between any pair of

122 nodes i and j is governed by its most efficient path. We denote with ϵ_{ij} the maximum efficiency of all

123 paths between i and j; its inverse is $d_{ij} = 1/\epsilon_{ij}$, the shortest electrical distance between i and j [40]. If

124 there is no connection between two nodes, i.e. if they are disconnected, ϵ_{ij} is set to zero. The shortest

125 paths for all node pairs in a weighted graph can be obtained efficiently through the Floyd-Warshall

126 algorithm [45].

127 The overall efficiency of the whole network is defined following Latora and Marchiori [29] as the sum

128 over all ϵ_{ij}:

$$E(G) = \frac{1}{N(N-1)} \sum_{i \neq j \in G} \epsilon_{ij} \tag{2}$$

129 2.2.2 *Cascading failure model*

130 Based on Motter and Lai [43], the cascading failure model describes the evolution of failures in the
131 network, considering the redistribution of loads in the network following initial line failures. In a first
132 step, the loads on the network lines are determined from the analysis of the intact network, i.e. at time 0.
133 The initial load $L_k(0)$ on a line k is defined as the total number of most efficient paths between any
134 node pair passing through that line [41, 43].

135 Each line k is characterized by a capacity C_k, which is proportional to its initial load:

$$C_k = \alpha \, L_k(0), k = 1,2, \dots, K, \tag{3}$$

136 where $\alpha \geq 1$ is the tolerance parameter of the network that quantifies the ratio of line capacity to the
137 initial line load. It corresponds to a safety factor of the network. In a real network, α might vary among
138 different lines.

139 Cascading failures are triggered by initial line failures. The interest here is in initial failures caused by
140 a natural hazard event, independent of the load and capacity of the lines. These initial failures are
141 reflected in an updated adjacency matrix **A**, in which the entries for all failed lines are set to zero. The
142 network is then re-analyzed with the updated adjacency matrix. In particular, the most efficient paths
143 among all node combinations are evaluated, and the new loads $L_k(1)$ in all lines $k = 1, \dots, K$ are
144 computed. It is assumed that overloaded lines fail, i.e. all lines for which $L_k(1) > C_k$ fail. The entries
145 in the adjacency matrix corresponding to these lines are set to zero, and the process is repeated until it
146 converges, i.e. until in one step no new line overloads occur.

147 Finally, the efficiency of the resulting (damaged) network is computed through Eq. (2). To obtain a
148 normalized measure of network damage, the efficiency of the damaged network is divided by the
149 efficiency of the intact network:

$$E_{norm} = \frac{E(G_{damaged})}{E(G)} \tag{4}$$

150 2.2.3 *Network reliability definition*

151 As described in the previous section, network performance is measured in terms of change in the overall
152 graph efficiency. A system failure event F_S is defined as the overall graph efficiency falling below a
153 threshold t_E. In this way, a binary system definition is introduced, with binary component and system
154 states:

$$F_S = \{E(G) < t_E\} \tag{5}$$

155 The system reliability is defined as

$$p_S = 1 - \Pr(F_S). \tag{6}$$

156 This binary definition provides only partial information on the system performance and it is dependent

157 on the definition of the t_E. It is introduced here to facilitate the use of classical reliability importance

158 measures.

159 **2.3 *Component importance***

160 We investigate the effect of spatial correlation in hazards on component importance rankings following

161 different importance measures (IMs). Classical reliability importance measures describe either how the

162 strengthening of individual components influences the system reliability, or they measure the impact of

163 component failures on system reliability [3, 6, 46]. Since the system performance is not inherently

164 binary, we include additionally an importance measure based on the effect of the component reliability

165 on the graph efficiency.

166 2.3.1 *Birnbaum's measure for a binary system*

167 The Birnbaum's measure (BM) describes the sensitivity of system reliability p_S to a change in the

168 component reliability $p_i = \Pr(X_i = 1)$:

$$
\begin{aligned}
BM_i &= \frac{\partial p_S}{\partial p_i} \\
&= \Pr(X_S = 1 | X_i = 1) - \Pr(X_S = 1 | X_i = 0)
\end{aligned} \tag{7}
$$

169 Following the second equality in Eq. (7), the BM can be computed as the difference between the

170 conditional probability that the system is functioning given component i is functioning and the

171 conditional probability that the system is functioning given component i has failed. This shows that BM

172 is independent of individual component reliability, which can be seen as a weakness of this IM [3].

173 However, the BM can be used to differentiate between those components that influence the system

174 reliability significantly and those that do not. The IM can thus serve to identify components of the

175 network worthy of further detailed investigation.

176 2.3.2 *Criticality importance for a binary system*

177 The criticality importance (CI) measure of a component i is the probability that failure of component i

178 is the cause of system failure, conditional on system failure having occurred. It can be defined as a

179 function of BM:

$$CI_i = \frac{BM_i \,(1 - p_i)}{1 - p_S} \tag{8}$$

180 While the BM is related mainly to the effect of increasing the component reliability, the CI includes the
181 ratio of component to system unreliability [3]. Based on CI rankings, a less reliable component is
182 deemed more critical.

183 ### 2.3.3 *Component importance based on graph efficiency sensitivity (ES)*

184 We additionally investigate an efficiency-based importance measure that does not require the definition
185 of a (binary) system failure event as for BM and CI. It describes the change in the expected value of the
186 overall graph efficiency with a change in the component failure probability:

$$ES_i = \frac{\partial \mathrm{E}[E_{norm}]}{\partial p_i} \tag{9}$$

187 By writing the expected value of the normalized efficiency as

$$\begin{aligned} \mathrm{E}[E_{norm}] = {}& \mathrm{E}[E_{norm}|X_i = 1]\Pr(X_i = 1) + \mathrm{E}[E_{norm}|X_i = 0]\Pr(X_i = 0) \\ = {}& \mathrm{E}[E_{norm}|X_i = 1]p_i + \mathrm{E}[E_{norm}|X_i = 0](1 - p_i), \end{aligned} \tag{10}$$

188 it is seen that the efficiency measure can be computed as

$$ES_i = \mathrm{E}[E_{norm}|X_i = 1] - \mathrm{E}[E_{norm}|X_i = 0]. \tag{11}$$

189 A deterministic version of this measure can be found in Latora and Marchiori [47], where the importance
190 of a component is measured in analogy to a (n-1)-contingency approach. They measure the decrease in
191 network efficiency after the component is removed from the graph.

192 ### 2.3.4 *Importance measures in cascading system failure events*

193 The above IM all include a derivation with respect to the component probability of failure. In cascading
194 system failure events triggered by (external) natural hazard events, it is relevant to distinguish (1) the
195 failures of components caused directly by the hazard event and (2) the failures of components caused
196 by the cascading effect. We refer to the former as the *initial component failures* and the latter as the
197 *cascading component failures.* Additionally, *final component failures* include both failure types.

198 All the above IM (as well as others) can be defined with respect to either of these three component
199 failure definitions. To distinguish these measures, we introduce the superscripts (i), (c) and (f) to
200 denote the IMs relating to initial, cascading and final component failures. Which of these IMs should be
201 used depends on the aim of the study. If the interest is in identifying components to be reinforced against
202 natural hazard events, the $CI^{(i)}$ or $ES^{(i)}$ should be employed. Conversely, $CI^{(c)}$ or $ES^{(c)}$ should be the
203 basis for identifying components for increasing capacity against overloading.

204 The measure of system performance employed in the IMs (either p_S or $\mathrm{E}[E_{norm}]$) should always relate
205 to the *final* performance of the system following the initial failures and the cascading effects.

2.4 *Generic hazard representation through a random field model of component failure probabilities*

In this contribution, a strongly idealized stochastic random field model is introduced for describing line failures originating from large scale natural hazards (e.g. wind loads). The model describes the component failure probabilities p_{F_k} of the lines during a hazard event through a random field. Let Z denote a standard normal random field, and Z_k its value at the midpoint of line k. The probability of failure of line k during the hazard event is obtained in function of Z_k through the following isoprobabilistic transformation:

$$p_{F_k} = F_{P_{F_k}}^{-1}[\Phi(Z_k)], \tag{12}$$

where Φ is the standard normal CDF and $F_{P_{F_k}}^{-1}$ is the inverse CDF of the component failure probability P_{F_k}. It is here modelled by the beta distribution, which is a common choice for characterizing probabilities.

In the above formulation, the spatial correlation between the failure probabilities at two locations k and l, p_{F_k} and p_{F_l}, is represented through the underlying standard Gaussian random field Z, by means of the following covariance function:

$$C_z(h) = \exp\left(-\frac{h^2}{r^2}\right), \tag{13}$$

where h [km] is the Euclidean distance between the locations of lines k and l, and r [km] is the correlation length. The correlation structure of the resulting beta random variables is approximately described by the autocorrelation function of Eq. (13); see also Der Kiureghian and Liu (1986).

Through variations of r, a range of different scenarios of hazard events can be modelled: from random and mutually independent failure events ($r = 0$), to large-scale fully correlated failure probabilities with spatially constant failure probabilities ($r = \infty$). The latter case reflects a situation in which the hazard is the same throughout the entire area, but the component failure events are still independent conditional on the hazard. When interpreting results for intermediate correlation lengths r, it is the relative value of r compared to the size of the infrastructure system that determines the system behavior.

The employed generic model with its one parameter (correlation length) is not able to address the specifics of a particular hazard type. Clearly, a spatial dependence model of a heat wave differs from that of a wind storm, and both are significantly more complex than the generic model used here. If desired, for specific hazards and network locations, parametric or numerical models can be employed instead, which more accurately reflect their specific dependence structure [11, 12, 48]. However, the use of specific hazard models impedes general conclusions. In particular, any specific spatially distributed hazard is described by a non-homogenous random field, and the effects of the change in the mean hazard

236 intensity are superimposed on the effects of dependence. This motivates the use of the simple generic

237 hazard model in this study.

3 NUMERICAL INVESTIGATIONS

3.1 *Implementation*

240 The case study is conducted for the IEEE 39 bus benchmark system for transmission power grids. It has

241 been designed to be representative of the New England transmission power network [49], and it was the

242 subject of a large number of studies [e.g., 50, 51]. The network consists of 39 buses including 10

243 generator buses, which are all modelled as leaf nodes. There are 46 transmission lines and transformers

244 in the network. By assigning coordinates to the nodes, the network is projected onto a hypothetical study

245 area of about 500 x 500 km^2 (Figure 1). The mean line length is 69 km, with a minimum of 25 km and

246 a maximum of 124 km. The graph efficiency value of the intact IEEE 39 network is 0.286.

247 Dwivedi, et al. [40] found that the IEEE 39 is a rather stable and reliable system. They conclude that the

248 system is robust with respect to random attacks; there is hardly any effect on the efficiency if lines are

249 randomly selected and removed.

250 The left-hand side of Figure 1 shows the lines weighted by their reactance values, and the right-hand

251 side of Figure 1 indicates the line capacities, which are proportional to the number of shortest paths

252 passing through the lines following Eq. (3). As expected, lines with lower reactance are more likely to

253 attract shortest paths, and vice versa.

254
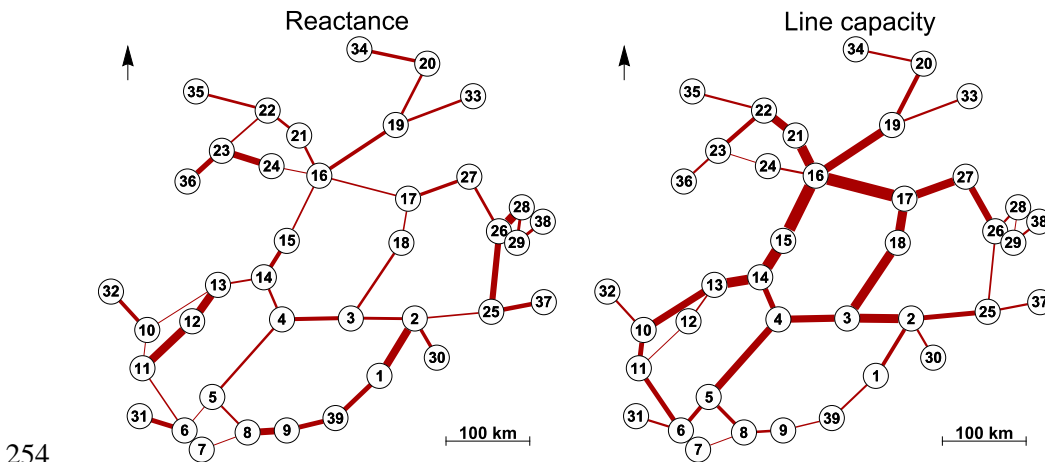
255 Figure 1: Plots of the IEEE 39 bus system with geo referenced nodes. Left: line thicknesses indicate the reactance values of the
256 lines; right: thicknesses indicate the line capacities, which are proportional to the number of shortest paths passing through the
257 lines.

258 We fix the mean component failure probability during a hazard event at 0.077 and its standard deviation

259 at 0.054. These values are motivated by an earlier study on hurricane impacts on component failure

260 probabilities and network damages in electrical transmission systems [48].

261   The correlation length r of the generic hazard model is varied to investigate the effect of spatial

262   correlation on system failure events, component importance, graph efficiency, and cascading depth, i.e.

263   mean number of cascading steps before the system stabilizes. Because an exact calculation of the

264   reliability of a general network with more than about 25 lines is an NP-hard problem [52], and because

265   we want to consider a variety of parameter constellations, our study is based on a Monte Carlo simulation

266   with at least 10^4 samples. All results are calculated with an efficiency threshold of $t_E = 0.9$ and a

267   tolerance parameter $\alpha = 1.5$, unless otherwise noted.

268   **3.2 Results**

269   *3.2.1 Spatial random field realizations*

270   Sample realizations of the spatial random field describing the component failure probability p_{F_i} for four

271   selected correlation length values are visualized in Figure 2. With increasing correlation length, random

272   field realizations are becoming increasingly homogeneous.
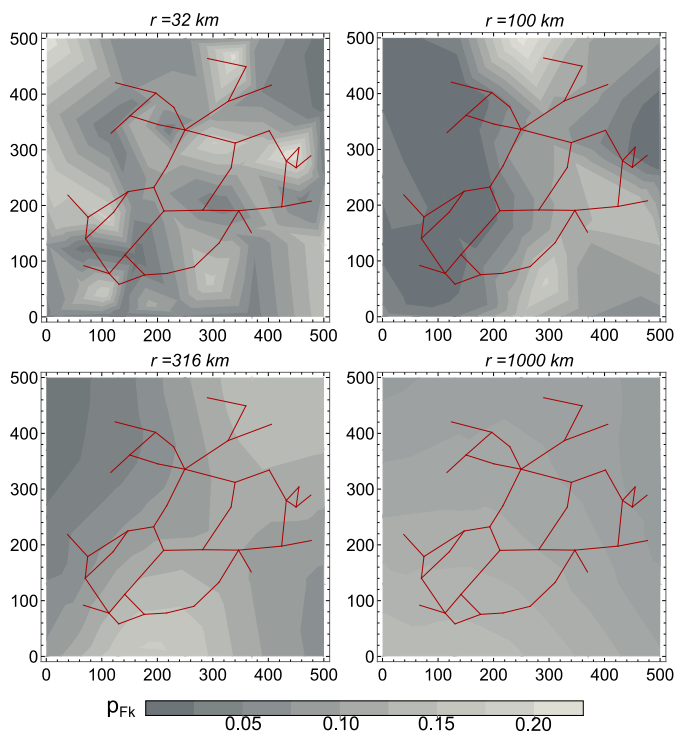
273

274   Figure 2: Spatial random field realizations of component failure probabilities for selected values of the correlation length,
275   together with the projected IEEE 39 bus system; scale unit is km.

276   *3.2.2 Network reliability as a function of the hazard correlation length*

277   The initially failed lines following a hazard event are compared with the number of finally failed lines

278   after the cascading process. In Figure 3 and Table 1, this comparison is performed for the case of

279   independent component failure probabilities ($r = 0$) and fully dependent component failure

280   probabilities ($r = \infty$). With increasing correlation length ($r \to \infty$), the variance of the number of

281   initially failed lines increases. This effect is weaker for the finally failed lines. The mean number of

initially failed lines is the same for all correlation lengths (by definition); however, the expected number of finally failed lines increases slightly with decreasing correlation length. This effect can be explained by the fact that the cascading failure process has the largest effect when just a few lines have failed initially, which is more probable with no or little dependence.
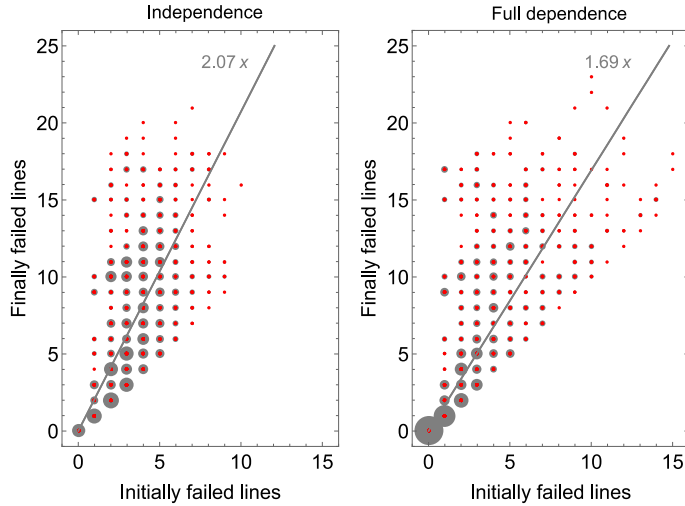
Figure 3: Finally versus initially failed lines for the case of independence (left) and full dependence (right); based on 10,000 samples with $\alpha = 1.5$; grey circles indicate the frequency of the data points in the sample space.

Table 1: Mean and standard deviation of the number of initially and finally failed lines; comparison of the independence and full dependence assumptions.

Failed lines	Parameter	Independence ($r = 0$)	Full dependence ($r = \infty$)
Initially	Mean	3.54	3.57
	Standard deviation	1.81	3.10
Finally	Mean	7.94	7.28
	Standard deviation	4.69	5.50

Means and standard deviations of graph efficiencies $E_{norm}(G_i)$ are shown in Figure 4, as a function of the correlation length r and the tolerance parameter α. The left-hand side of Figure 4 shows that the overall graph efficiency is increasing with the correlation length r. This result, which may at first glance appear counterintuitive, is consistent with the effect shown in Figure 3. With increasing correlation length it is more likely that no line failures or a larger number of line failures occur initially; in both cases, cascading processes will be attenuated or will not be triggered at all. The vulnerability of the system is larger for small values of α. For systems with limited vulnerability (α larger than 3.0), the correlation length has only a weak effect on the mean efficiency following the hazard, because cascading effects are limited.

The standard deviation of the efficiency increases significantly with increasing correlation length (Figure 4 right). This can be explained with the increasing variance in the component failure probability, which is observed for higher values of r (compare with Figure 3 and Table 1).

303 Changes in the mean and standard deviation occur mainly in the range $100-1000 \text{ km}$, which
304 corresponds to the order of magnitude of the network size. For correlation lengths smaller than 100 km,
305 the behavior is similar to the uncorrelated case, whereas for correlation lengths larger than 1000 km, it
306 approaches that of the fully correlated case. The results for small correlation lengths are affected by the
307 simplified discretization of the lines, in which the failure probability of the lines is evaluated at the line
308 midpoints. When considering the distributed nature of the lines, the failure probabilities of the individual
309 lines would increase with decreasing correlation.
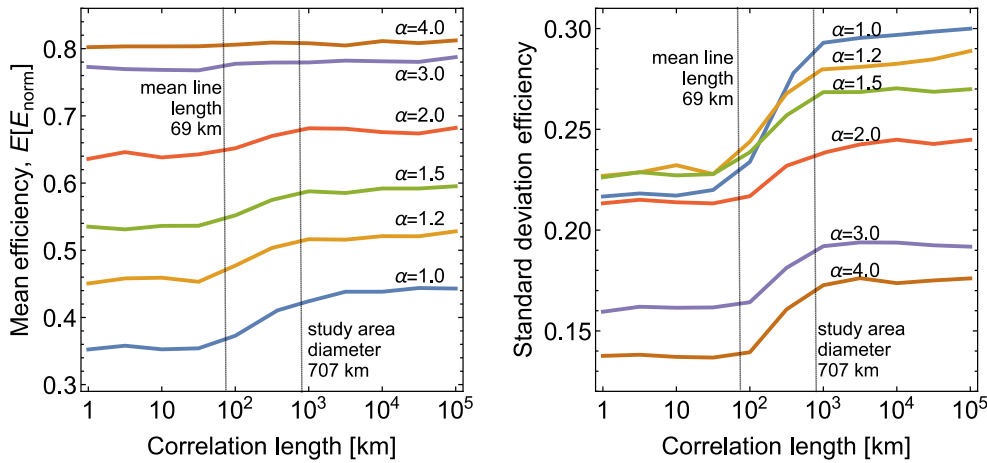
310

311 Figure 4: Network performance as function of the correlation length with varying α value. Left: mean overall graph
312 efficiency $E[E_{norm}]$; right: standard deviation of overall graph efficiency; based on 10,000 samples per correlation length value
313 and α value combinations.

3.2.3 *Component importance rankings*

315 Figure 5 visualizes the criticality importance (CI) with respect to initial failures ($CI^{(i)}$) and cascading
316 failures ($CI^{(c)}$) for a correlation length of 100 km. The two rankings differ significantly, indicating that
317 lines that are important for the initialization of network damage do not correspond to the lines that are
318 responsible for the further propagation of cascading overloads. Initial line failures are most important in
319 lines which are centrally located in the network graph and which have high initial loads. Cascading
320 failures are most important in lines with low initial load and capacity, as these are more likely to be
321 overloaded (see Figure 1). As expected, leaf lines are ranked as the least important ones, for initial as
322 well as cascading failure. The resulting $CI^{(f)}$ values are close to the $CI^{(c)}$ values in the right-hand side
323 of Figure 5 and are therefore not depicted here. BM importance measures lead to a ranking very similar
324 to CI, these results are also omitted here.
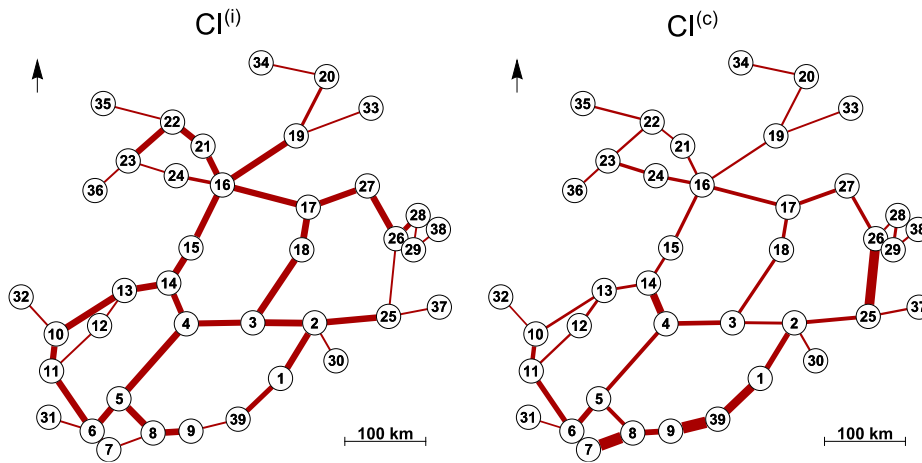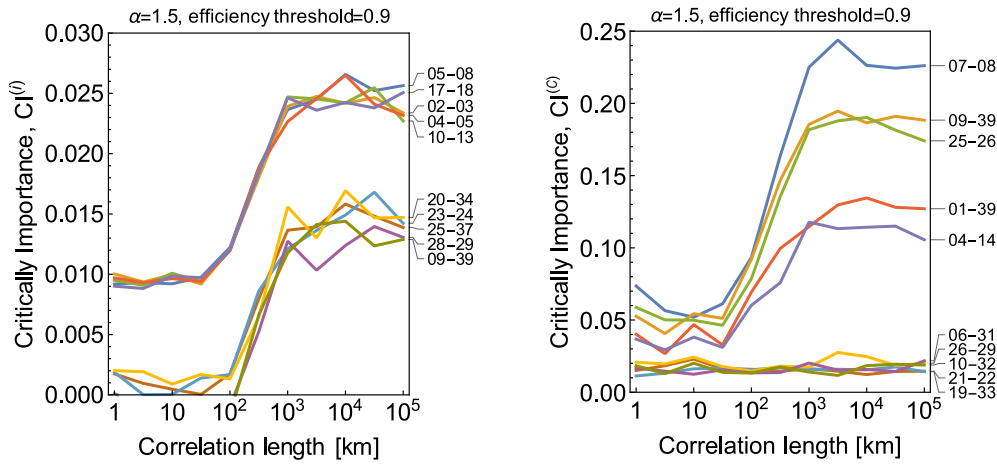
Figure 5: CI weighted graph at a correlation length of 100 km. Left: $CI^{(i)}$ with respect to initial failures; right: $CI^{(c)}$ with respect to cascading failures; with $\alpha = 1.5$ and $t_E = 0.9$; based on 10,000 samples.

In Figure 6, ES importance measures are summarized. Overall, these show a similar pattern as the CI of Figure 5. The network topology determines the $ES^{(i)}$ ranking; lines with a bypass are lower ranked, lines without bypass are in the middle range, and lines that link clusters with each other are highly ranked. The important lines with respect to cascading failures, i.e. the $ES^{(c)}$ values, are more uniformly distributed in the network. This effect is similar to the difference between $CI^{(i)}$ and $CI^{(c)}$.
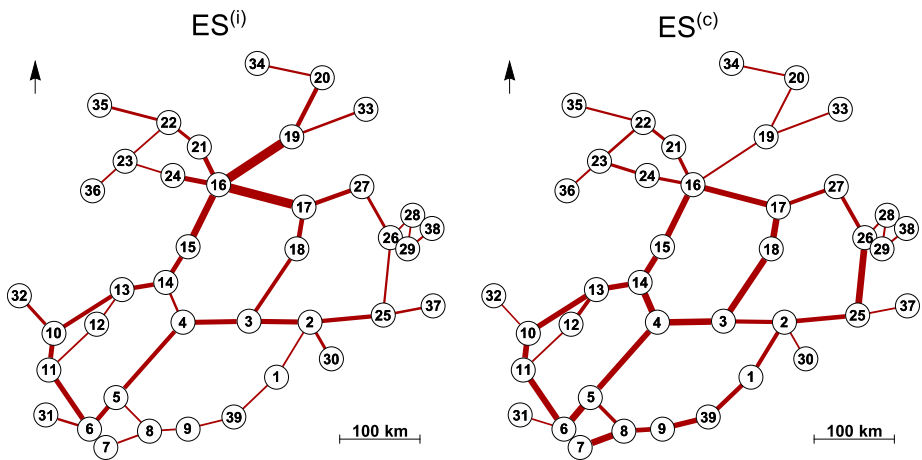
Figure 6: ES importance weighted graph at a correlation length of 100 km. Left: $ES^{(i)}$ with respect to initial failures; right: $ES^{(c)}$ with respect to cascading failures; with $\alpha = 1.5$; based on 10,000 samples.

We also compared the IM values to the betweenness index as shown in Figure 1, as an example of a topological measure. Whereas the betweenness index exhibits correlation coefficients in the order of 0.70 with $ES^{(i)}$ and $CI^{(i)}$, its dependence with $CI^{(c)}$ and $ES^{(c)}$ is significantly less pronounced. These results indicate that the purely topological betweenness index is only partially suitable as a proxy for IMs based on the system performance.

Figure 7 shows the effect of the hazard correlation length on CI component importance rankings. While the values of $CI^{(i)}$ and $CI^{(c)}$ change significantly with varying correlation length, their respective rankings change only slightly. As in Figure 4, changes in CI occur mainly in the range $100 - 1000$ km,

corresponding to the network size. The five to ten highest ranked lines are essentially the same, independent of the variation in the correlation length. The difference in the rankings of $CI^{(i)}$ to those of $CI^{(c)}$ reflect the differences observable in Figure 5. As an example, line 9-39 is low ranked in importance with respect to failures caused by the hazard, but highly ranked in importance with respect to the cascading failure process.

Figure 7: CI as function of correlation length. Left: $CI^{(i)}$ with respect to initial failures; right: $CI^{(c)}$ with respect to cascading failures; with $\alpha = 1.5$ and $t_E = 0.9$ each and based on 10,000 samples per correlation length value.

It is found that the rankings based on $CI^{(f)}$ are close to those based on $CI^{(c)}$ and are therefore not depicted here. Furthermore, BM and CI deliver similar results, and the five most important components coincide. The CI is based on the BM, while it additionally includes the reliability of the individual components. Here, CI is similar to BM because the component reliabilities with respect to hazardous extrinsic impacts are identical. This is not the case after cascading failure processes: a lower correlation between $BM^{(c)}$ and $CI^{(c)}$ is observed in comparison to that between $BM^{(i)}$ and $CI^{(i)}$.

Figure 8 depicts the rankings based on $ES^{(i)}$ and $ES^{(c)}$. The pattern is similar to the one of CI and BM, even though different lines are identified as the most important ones.
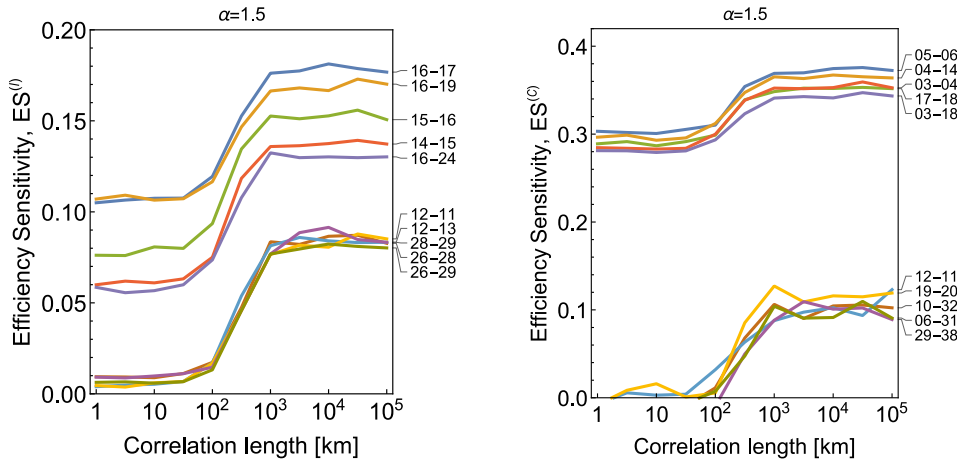
Figure 8: ES as function of correlation length. Left: $ES^{(i)}$ with respect to initial failures; right: $ES^{(c)}$ with respect to cascading failures; with $\alpha = 1.5$ each and based on 10,000 samples per correlation length value.

363 As Tanguy [27] observes in his study on general CCF models and their influence on importance
364 measures, adding CCF effects to the description of the IEEE system does not profoundly change the
365 ranking of the lines when comparing to the independence assumption for all components. Our results
366 indicate that this also holds in essence for spatial correlation effects under consideration of cascading
367 failure processes.

368 In addition, we assessed the sensitivity of the results to changes in the tolerance parameter α and the
369 efficiency threshold t_E utilized in the definition of system failure. For vulnerable systems (e.g., $\alpha < 2$
370 and $t_E > 0.7$), we find that the IM values are sensitive to the correlation length. In contrast, for less
371 vulnerable systems (e.g., $\alpha > 2$ and $t_E < 0.5$), the change of the IM values with the correlation length
372 is less pronounced. In all cases, the ranking remained consistent among different correlation lengths.

373 3.2.4 *Results for IEEE118*
374 Additional numerical investigations were performed on the larger IEEE 118 network [49]. We do not
375 report the results in detail, because they are consistent with the results obtained for the IEEE 39 network.
376 The dependence of network reliability on hazard correlation length in the IEEE 118 exhibits the same
377 trends as presented above. The clear distinction between the initial component importance rankings
378 ($CI^{(i)}, ES^{(i)}$) and the cascading component importance rankings ($CI^{(c)}, ES^{(c)}$) is also observed for
379 IEEE118.

380 **3.3 *Strategies for improving network performance under hazards***

381 Ultimately, the IMs should support decision making. To this end, we investigate network improvement
382 strategies based on the proposed IMs, by measuring the effect of strengthening or increasing capacity of
383 selected lines on the network overall efficiency of the IEEE 39 network. Two network improvement
384 strategies are considered:

385 1) Line strengthening of the five most important lines ranked by either $CI^{(i)}$ or $ES^{(i)}$, corresponding to
386 an increase in the resistance against the hazardous (wind) load. Line strengthening is modeled by
387 reducing the initial line failure probability to 10% of its original value.

388 2) Increase of the line capacity of the five most important lines ranked by either $CI^{(c)}$ or $ES^{(c)}$,
389 corresponding to an increase in the resistance of the lines against overloading in the cascading failure
390 process. The capacity increase is modeled by increasing the tolerance parameter α by a factor of three.

391 In Figure 9, we compare the resulting mean efficiency in function of the hazard correlation length. The
392 results in Figure 9 (left) show that strengthening lines according to $ES^{(i)}$ and $CI^{(i)}$ rankings lead to
393 similarly increased mean efficiencies, even though the rankings of the two measures do not coincide in
394 their respective five highest ranked lines. For comparison, we also compute the resulting mean efficiency

395 when lines are selected for strengthening following the $ES^{(c)}$ and $CI^{(c)}$ ranking. Such a strengthening

396 of lines does not significantly affect the system performance, highlighting the suitability of $ES^{(i)}$

397 and $CI^{(i)}$ rankings for prioritizing network components for strengthening against hazard impacts.

398 Figure 9 (right) shows that the largest improvement of the resulting mean efficiency from increasing

399 line capacity is obtained by selecting components according to $ES^{(c)}$. The ranking based on $CI^{(c)}$ leads

400 to significantly lower gain in mean efficiency. As expected, $ES^{(i)}$ and $CI^{(i)}$ rankings are not suitable for

401 identifying components for line capacity increase.
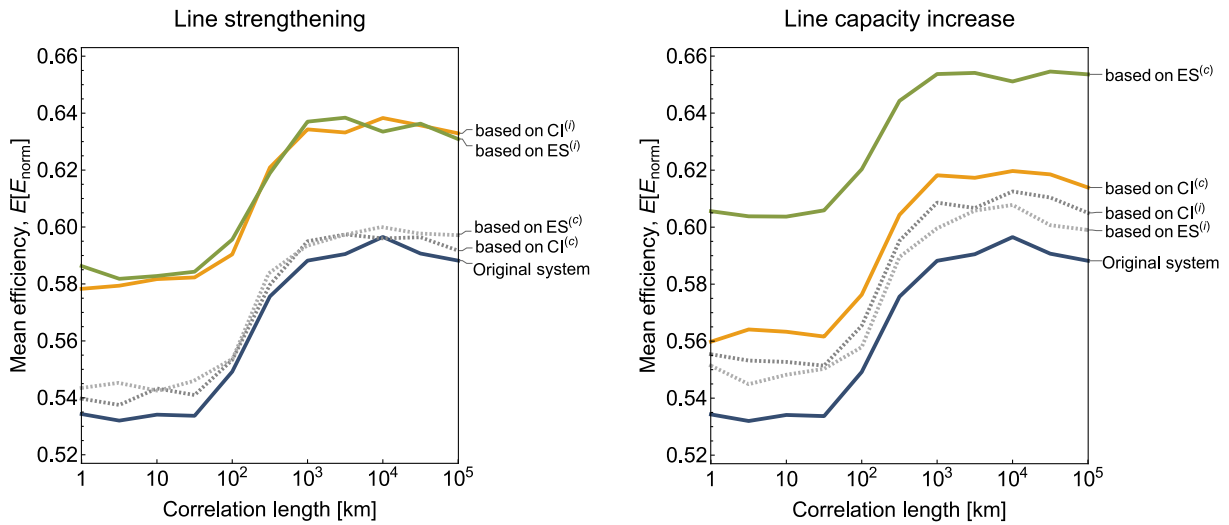
402

403 Figure 9: Mean efficiency in function of correlation length for different network improvement strategies. Left: line
404 strengthening (decreasing the initial failure probability during the hazard event) of five selected lines; right: increasing line
405 capacity (increasing the tolerance parameter α) of five selected lines.

4 CONCLUSION

407 This study is a contribution to a fast, preliminary reliability assessment of large infrastructure networks.

408 Its aim is an improved understanding of the importance of components in a network under large-scale

409 spatially dependent hazards and internal cascading failure processes in the network. The well-known

410 and widely used efficiency measure by Latora and Marchiori [29] and the model for cascading failure

411 by Crucitti, et al. [41] have been implemented.

412 To address the specifics of the cascading failure process, we propose the use of separate importance

413 measures, considering on the one hand initial (triggering) component failures caused directly by the

414 hazard event, and on the other hand cascading component failures. This differentiation reflects the fact

415 that different measures are necessary for increasing component reliability with respect to the two failure

416 modes. As our results show, the component importance rankings differ significantly between the two

417 strategies. The importance of lines with respect to failures caused by the initial hazard is related to their

418 initial capacity (compare Figure 6 with Figure 1). The components that are of largest importance for the

419 cascading process are lines with smaller capacity, which are located parallel to lines with the highest

420   capacities. In both cases, the lines identified as the most important ones differ significantly from the
421   ranking based solely on a topological measure such as the betweenness index shown in Figure 1.
422   An application of the proposed importance measures for selecting lines for strengthening or capacity
423   increase demonstrated their suitability for defining network improvement strategies.

424   The overall reliability is affected by the spatial dependence of the hazard process. Our study shows that
425   an increasing spatial dependence, as expressed by the correlation length, leads on average to smaller
426   system failure events (if the mean failure rate in the lines is fixed). This result appears counterintuitive
427   because in reality larger spatial dependence is often associated with overall larger failure rates, which
428   however are kept constant for all correlation lengths in our study. In contrast to the network reliability,
429   none of the component importance rankings is noticeably affected by the dependence structure. This
430   seems to indicate that component importance analysis can be performed without considering the spatial
431   dependence explicitly. However, in the analysis of a real system, the change in the mean failure rate
432   with spatial location must be included, hence a detailed analysis of the hazard is nevertheless necessary.

5 ACKNOWLEDGEMENTS

6 LITERATURE

438 [1]   M. Bruch, V. Münch, M. Aichinger, M. Kuhn, M. Weymann, and S. Gerhard, "Power Blackout
439   Risks - Risk Management Options," CRO Forum2011.
440 [2]   N. Hodge. (2012, Emerging risks on the horizon - Energy Risk. *Global Risk Dialogue (Spring*
441   *Issue 2012),* 28-33.
442 [3]   M. Rausand and A. Høyland, *System Reliability Theory Models, Statsitical Methods, and*
443   *Applications*, Second Edition ed. New Jersey: John Wiley & Sons. Inc., 2004.
444 [4]   W. Wang, J. Loman, and P. Vassiliou, "Reliability importance of components in a complex
445   system," presented at the Proceedings of the Reliability and Maintainability Annual
446   Symposium, RAMS 2004, 2004.
447 [5]   P. Hilber and L. Bertling, "Component reliability importance indices for electrical networks,"
448   presented at the International Conference on Power Engineering, IPEC Singapore, 2007.
449 [6]   T. Daemi and A. Ebrahimi, "Evaluation of Components Reliability Importance Measures of
450   Electric Transmission Systems Using the Bayesian Network," *Electric Power Components and*
451   *Systems,* vol. 40, pp. 1377-1389, 2012/08/15 2012.
452 [7]   J. F. Espiritu, D. W. Coit, and U. Prakash, "Component criticality importance measures for the
453   power industry," *Electric Power Systems Research,* vol. 77, pp. 407-420, 4// 2007.
454 [8]   F. Cadini, E. Zio, and C.-A. Petrescu, "Using Centrality Measures to Rank the Importance of
455   the Components of a Complex Network Infrastructure," in *Critical Information Infrastructure*
456   *Security: Third International Workshop, CRITIS 2008, Rome, Italy, October13-15, 2008.*
457   *Revised Papers*, R. Setola and S. Geretshuber, Eds., ed Berlin, Heidelberg: Springer 2009, pp.
458   155-167.

[9]   E. Zio and R. Piccinelli, "Randomized flow model and centrality measure for electrical power transmission network analysis," *Reliability Engineering & System Safety,* vol. 95, pp. 379-385, 2010.

[10] L. Dueñas-Osorio, "Interdependent Response of Networked Systems to Natural Hazards and Intentional Disruptions," PhD thesis, School of Civil and Environmental Engineering, Georgia Institute of Technology, 2005.

[11] M. Ouyang and L. Dueñas-Osorio, "Multi-dimensional hurricane resilience assessment of electric power systems," *Structural Safety,* vol. 48, pp. 15-24, 5// 2014.

[12] J. Winkler, L. Dueñas-Osorio, R. Stein, and D. Subramanian, "Performance assessment of topologically diverse power systems subjected to hurricane events," *Reliability Engineering & System Safety,* vol. 95, pp. 323-336, 4// 2010.

[13] T. Adachi, "Impact of Cascading Failures on Performance Assessment of Civil Infrastructure Systems," PhD thesis, School of Civil and Environmental Engineering, Georgia Institute of Technology, Georgia, 2007.

[14] A. Mosleh, K. N. Fleming, G. W. Parry, H. M. Paula, D. H. Worledge, and D. M. Rasmuson, "Procedures for treating common cause failures in safety and reliability studies: procedural framework and examples," U.S. Nuclear Regulatory Commission, Newport Beach, CA1988.

[15] A. Mosleh, "Common cause failures: An analysis methodology and examples," *Reliability Engineering & System Safety,* vol. 34, pp. 249-292, 1991/01/01 1991.

[16] J. K. Vaurio, "An implicit method for incorporating common-cause failures in system analysis," *Reliability, IEEE Transactions on,* vol. 47, pp. 173-180, 1998.

[17] W. Dongwei, Da Huo, L. GuiQing, and C. YianYian, "Reliability Analysis of Lifline Networks with Vertex and Correlation Failures," presented at the Eleventh World Conference on Earthquake Engineering, Acapulco, Mexico, 1996.

[18] M. Javanbarg, C. Scawthorn, J. Kiyono, and Y. Ono, "Multi-Hazard Reliability Analysis of Lifeline Networks," in *TCLEE 2009*, ed: American Society of Civil Engineers, 2009, pp. 1-8.

[19] H.-W. Lim and J. Song, "Efficient risk assessment of lifeline networks under spatially correlated ground motions using selective recursive decomposition algorithm," *Earthquake Engineering & Structural Dynamics,* vol. 41, pp. 1861-1882, 2012.

[20] S. Neumayer and E. Modiano, "Network Reliability with Geographically Correlated Failures," in *INFOCOM, 2010 Proceedings IEEE*, 2010, pp. 1-9.

[21] S. Neumayer, G. Zussman, R. Cohen, and E. Modiano, "Assessing the impact of geographically correlated network failures," in *MILCOM 2008 - 2008 IEEE Military Communications Conference*, 2008, pp. 1-6.

[22] P. K. Agarwal, A. Efrat, S. K. Ganjugunte, D. Hay, S. Sankararaman, and G. Zussman, "Network vulnerability to single, multiple, and probabilistic physical attacks," in *Military Communications Conference, 2010 - Milcom 2010*, 2010, pp. 1824-1829.

[23] A. Bernstein, D. Bienstock, D. Hay, M. Uzunoglu, and G. Zussman, "Power grid vulnerability to geographically correlated failures - Analysis and control implications," in *IEEE INFOCOM 2014 - IEEE Conference on Computer Communications*, 2014, pp. 2634-2642.

[24] M. Andreasson, S. Amin, and K. H. Johansson, "Correlated Failures of Power Systems: Analysis of the Nordic Grid," presented at the Workshop on Foundations of Dependable and Secure Cyber-Physical Systems (FDSCPS), Chicago, Illinois, 2011.

[25] M. Rahnamay-Naeini, J. E. Pezoa, G. Azar, N. Ghani, and M. M. Hayat, "Modeling Stochastic Correlated Failures and their Effects on Network Reliability," in *Computer Communications and Networks (ICCCN), 2011 Proceedings of 20th International Conference on*, 2011, pp. 1-6.

[26] C. Bérenguer, L. Dieulle, A. Grall, and D. Vasseur, "Études de sensibilité, facteurs d'importance et défaillances de cause commune " *Journal Européen des Systèmes Automatisés,* vol. 40, pp. 763-785, 2006.

[27] C. Tanguy, "Importance measures and common-cause failure in network reliability," in *European Safety and Reliability Conference, ESREL*, Troyes, France, 2011.

[28] A. Scherb, L. Garrè, Y. Yang, and D. Straub, "Component importance in infrastructure networks subject to spatially distributed hazards," in *European Safety and Reliability, ESREL 2016*, Glasgow, 2016.

[29] V. Latora and M. Marchiori, "Efficient Behavior of Small-World Networks," *Physical Review Letters,* vol. 87, p. 198701, 10/17/ 2001.

515   [30]   Z. Wang, A. Scaglione, and R. J. Thomas, "Electrical centrality measures for electric power grid
516   vulnerability analysis," in *49th IEEE Conference on Decision and Control (CDC)*, 2010, pp.
517   5792-5797.
518   [31]   M. Rosas-Casals, S. Valverde, and R. V. SolÉ, "Topological Vulnerability of the European
519   Power Grid under Errors and Attacks," *International Journal of Bifurcation and Chaos,* vol. 17,
520   pp. 2465-2475, 2007/07/01 2007.
521   [32]   S. Arianos, E. Bompard, A. Carbone, and F. Xue, "Power grid vulnerability: A complex network
522   approach," *Chaos,* vol. 19, p. 013119, 2009.
523   [33]   P. Crucitti, V. Latora, and M. Marchiori, "Locating Critical Lines in High-Voltage Electrical
524   Power Grids," *Fluctuation and Noise Letters,* vol. 05, pp. L201-L208, 2005/06/01 2005.
525   [34]   P. Hines, E. Cotilla-Sanchez, and S. Blumsack, "Do topological models provide good
526   information about electricity infrastructure vulnerability?," *Chaos,* vol. 20, p. 033122, 2010.
527   [35]   D. P. Chassin and C. Posse, "Evaluating North American electric grid reliability using the
528   Barabási–Albert network model," *Physica A: Statistical Mechanics and its Applications,* vol.
529   355, pp. 667-677, 9/15/ 2005.
530   [36]   R. V. Solé, M. Rosas-Casals, B. Corominas-Murtra, and S. Valverde, "Robustness of the
531   European power grids under intentional attack," *Physical Review E,* vol. 77, p. 026102, 02/07/
532   2008.
533   [37]   E. Bompard, R. Napoli, and F. Xue, "Analysis of structural vulnerabilities in power transmission
534   grids," *International Journal of Critical Infrastructure Protection,* vol. 2, pp. 5-12, 5// 2009.
535   [38]   G. A. Pagani and M. Aiello, "The Power Grid as a complex network: A survey," *Physica A:*
536   *Statistical Mechanics and its Applications,* vol. 392, pp. 2688-2700, 6/1/ 2013.
537   [39]   F. Saccomanno, *Electric power systems*. Piscataway, NJ: IEEE Press, 2003.
538   [40]   A. Dwivedi, X. Yu, and P. Sokolowski, "Identifying vulnerable lines in a power network using
539   complex network theory," in *2009 IEEE International Symposium on Industrial Electronics*,
540   2009, pp. 18-23.
541   [41]   P. Crucitti, V. Latora, and M. Marchiori, "Model for cascading failures in complex networks,"
542   *Physical Review E,* vol. 69, p. 045104, 04/29/ 2004.
543   [42]   R. Albert, I. Albert, and G. L. Nakarado, "Structural vulnerability of the North American power
544   grid," *Physical Review E,* vol. 69, p. 025103, 02/26/ 2004.
545   [43]   A. E. Motter and Y.-C. Lai, "Cascade-based attacks on complex networks," *Physical Review E,*
546   vol. 66, p. 065102, 12/20/ 2002.
547   [44]   P. Crucitti, V. Latora, and M. Marchiori, "A topological analysis of the Italian electric power
548   grid," *Physica A: Statistical Mechanics and its Applications,* vol. 338, pp. 92-97, 7/1/ 2004.
549   [45]   R. W. Floyd, "Algorithm 97: Shortest path," *Commun. ACM,* vol. 5, p. 345, 1962.
550   [46]   W. E. Vesely, T. C. Davis, R. S. Denning, and N. Saltos, "Measures of risk importance and their
551   applications.," US Nuclear Regulatory Commission1983.
552   [47]   V. Latora and M. Marchiori, "How the science of complex networks can help developing
553   strategies against terrorism," *Chaos, Solitons & Fractals,* vol. 20, pp. 69-75, 4// 2004.
554   [48]   A. Scherb, L. Garrè, and D. Straub, "Probabilistic Risk Assessment of Infrastructure Networks
555   Subjected to Hurricanes," in *12th International Conference on Applications of Statistics and
556   Probability in Civil Engineering, ICASP12*, Vancouver, 2015.
557   [49]   R. Christie, "Power Systems Test Case Archive," ed. Washington: Electrical Engineering
558   Department, University of Washington, 2000.
559   [50]   C. North American Rockwell, I. Edison Electric, and I. Electric Power Research, *On-line
560   stability analysis study RP90-1, October 12, 1970*. Palo Alto, Calif.: Electric Power Research
561   Institute, 1970.
562   [51]   T. Athay, R. Podmore, and S. Virmani, "A Practical Method for the Direct Analysis of Transient
563   Stability," *IEEE Transactions on Power Apparatus and Systems,* vol. PAS-98, pp. 573-584,
564   1979.
565   [52]   J. C. Whitson and J. E. Ramirez-Marquez, "Resiliency as a component importance measure in
566   network reliability," *Reliability Engineering & System Safety,* vol. 94, pp. 1685-1693, 10// 2009.

7 LIST OF FIGURES

8 LIST OF TABLES